AJNR

MR demonstration of altered cerebrospinal fluid flow by obstructive lesions.

J L Sherman, C M Citrin, B J Bowen and R E Gangarosa

AJNR Am J Neuroradiol 1986, 7 (4) 571-579
http://www.ajnr.org/content/7/4/571

MR Demonstration of Altered Cerebrospinal Fluid Flow by Obstructive Lesions

John L. Sherman[1,2,3]
Charles M. Citrin[1,3]
Bruce J. Bowen[1]
Raymond E. Gangarosa[4]

We investigated the MR imaging appearance of flowing cerebrospinal fluid (CSF) in the brain in the presence of obstructive lesions of the ventricular pathways. The pulsatile movement of CSF through the ventricular system is seen as an area of low signal intensity that has been termed the CSF flow-void sign (CFVS). This is best appreciated in areas of narrowing within the ventricular system; that is, the aqueduct of Sylvius, foramen of Magendie, and interventricular foramina. MR studies of 27 patients with lesions affecting the ventricular pathways were reviewed for the presence of the CFVS. Single-echo T1-weighted and T2-weighted multisection techniques were used in all cases. The CFVS was always seen more prominently on the T2-weighted images. The presence of the CFVS indicated patency of the ventricular pathway in which it was identified. The absence of the CFVS in the presence of hydrocephalus indicated that a possible obstructive lesion was present, but it did not directly indicate the level of the obstruction. The CFVS was absent in the aqueduct of Sylvius in 13 patients with obstruction or stenosis of the aqueduct, but it was also absent in one patient with a colloid cyst of the interventricular foramina. In three patients with preoperative and postoperative MR, the CFVS was seen in the area of interest only after resection of the obstructing lesion. We concluded that the presence of the CFVS is a useful indicator of the patency of the ventricular pathway in which it is seen. The absence of the CFVS at a location in which it is normally seen may indicate the presence of an obstruction, but it must be correlated with other signs to be interpreted correctly.

Cerebrospinal fluid (CSF) has a variable intensity, depending on its state of motion [1–3]. On T2-weighted spin-echo pulse sequences the CSF in the lateral ventricles appears hyperintense relative to brain, while CSF in the narrower areas of the ventricular system often has a decreased intensity. The decreased intensity is caused by CSF motion and has been termed the CSF flow-void sign (CFVS) [1, 2]. Our purpose is to study the usefulness of the CFVS in evaluating obstructive lesions of the ventricular pathways.

Subjects and Methods

The MR imaging of 27 patients with lesions causing mass effect on intracranial cerebrospinal fluid (CSF) pathways were evaluated retrospectively. These patients were selected by reviewing the files for cases in which masses or other lesions affected localized areas of the ventricular system. We sought patients in which the compressive effects were limited to one of the following areas: the foramina of Monro, the anterior third ventricle, the posterior third ventricle, the aqueduct of Sylvius, the body of the fourth ventricle, and the fourth ventricular outlet foramina. Patients were separated into three groups depending on the level of the lesion. The effect of the lesion on CSF pathways was determined. The CFVS was specifically identified and its location recorded. The severity of the ventriculomegaly was measured using the ventricular size index and categorized as mild, moderate, or severe [4] (see criteria in Table 1). Correlation with operative findings, postoperative MR and computed tomography (CT) scans, and clinical course was made.

Group 1 included six patients with mass effect at the level of the foramina of Monro or

Received October 18, 1985; accepted after revision February 12, 1986.

[1] Magnetic Imaging of Washington, 5550 Friendship Blvd., Chevy Chase, MD 20815. Address reprint requests to J. L. Sherman.

[2] Uniformed Services University of the Health Sciences, Bethesda, MD 20814.

[3] George Washington University School of Medicine, Washington, D.C. 20037.

[4] Clinical Science Center, Picker International, 5500 Avion Park Dr., Highland Heights, OH 44143.

AJNR 7:571–579, July/August 1986
0195–6108/86/0704–0571

TABLE 1: **Ventricular Size Index**

Severity	%
Normal	30 or less
Mild	30–39
Moderate	40–46
Severe	47 or more

Note.—Ratio of the distance between the lateral margins of the frontal horns to the distance between the inner tables of skull at the same level.

third ventricle. There were two patients with colloid cysts obstructing the foramina of Monro, three patients with gliomas of the hypothalamic area, and one patient with a meningioma with suprasellar extension.

Group 2 included 13 patients with obstructing lesions of the aqueduct of Sylvius. There were seven patients with aqueductal stenosis, four of whom were shunted during childhood, and three patients who presented as adults. Four patients had presumed tumors of the mesencephalon, one patient had a thalamic glioma, and one patient had sarcoidosis with aqueductal obstruction.

Group 3 included eight patients with compression or distortion of the fourth ventricle. The lesions responsible for the mass effect included one each of a brainstem glioma, a choroid plexus papilloma, an intraventricular astrocytoma, a cerebellar hemangioblastoma, and an acoustic neuroma. Two patients had a metastasis to the cerebellum. One patient with fourth ventricular compression due to a Chiari malformation was also included, although the true level of obstruction has not been definitely determined.

MR examinations were performed using a Picker Vista (Cleveland, OH) MR superconductive 0.5 T imager. Standard manufacturer-provided pulse sequences and reconstruction algorithms were employed, without cardiac gating. Data were typically acquired with 256 complex samples/views, 256 views, and two excitations using the two-dimensional Fourier transform (2D FT) method and spin-echo (SE) pulse sequences. The resultant 256 × 256 image was then interpolated to a 512-element display matrix. Field-of-view for these examinations was 25 or 30 cm, resulting in a pixel size (before interpolation) of 0.98 × 0.98 mm or 1.17 × 1.17 mm. Sampling times were 24 msec, and sampling band width was 5 KHz. Single-echo eight or 16 multisection SE sequences were performed with selective excitation in staggered slice order by exciting odd-number slices sequentially followed by even-number slices sequentially. Slices were contiguous and either 5 or 10 mm thick. Slice profiles were approximately trapezoidal, with 1-mm transitional zones on either side of a flat region of the nominal thickness [5]. The phase-encoding gradient was horizontal in all cases.

T2-weighted and T1-weighted sequences were used in all cases. T2-weighted sequences were obtained with a TE of 60, 80, or 100 msec and a TR of 1500–4000 msec. T1-weighted sequences used a TE of 30 or 40 msec, with a TR of 500–600 msec. The CSF in the lateral ventricles appears hyperintense relative to cerebral cortex on the T2-weighted sequences, and hypointense on the T1-weighted sequences. In some cases, additional sequences were added to the basic examination. Slice-to-slice variability in contrast was not significant in any pulse sequences.

Results

General

In many cases T2-weighted images were available in two projections, axial and coronal or axial and sagittal. While a formal analysis of the differences between images in different projections was not performed, we noted that when the CFVS was visible in one projection it was also visible in the other projection if the image section thickness was equal for both. Midline sagittal images were usually preferred since they allowed visualization of the third ventricle, aqueduct of Sylvius, and fourth ventricle in a single section. Coronal images were not as good as sagittal or transaxial images for visualization of the aqueduct because the structures of interest were not completely in the plane of the image. Familiarity with the anatomical relationships was the main advantage to the axial projection.

In four patients in whom both 5- and 10-mm thick sections were available using comparable T2-weighted sequences in the same plane, we noted slightly better visualization of the CFVS on the 5-mm thick sections in three patients; and in one case, the CFVS was visible only on the 5-mm thick sections.

Group 1. Six Patients with Lesions of the Interventricular Foramina or the Third Ventricle

All six patients had hydrocephalus confined to the lateral ventricles. The two patients with colloid cysts and two of the patients with hypothalamic gliomas obstructing the anterior third ventricle and interventricular foramina had interstitial edema.

In one patient with an 11-mm colloid cyst, the CFVS was present only in the caudal fourth ventricle and foramen of Magendie. After surgical removal of the colloid cyst, the hydrocephalus and interstitial edema resolved. Repeat MR with identical pulse sequences revealed the CFVS coursing from the interventricular foramina through the third ventricle, aqueduct of Sylvius, fourth ventricle, and foramen of Magendie (Fig. 1).

In the second patient with a colloid cyst, the CFVS was present in the aqueduct of Sylvius despite the obstruction at the interventricular foramina. Hydrocephalus of the lateral ventricles was more severe in this patient than in the prior patient with a colloid cyst. Two of the three patients with tumors of the hypothalamic area had moderate hydrocephalus and one had severe hydrocephalus due to obstruction of the anterior third ventricle and interventricular foramina (Fig. 2). The CFVS was visible only in the fourth ventricle in all three of these patients. The patient with a meningioma bulging into the anterior third ventricle had moderate ventriculomegaly; however, the CFVS was present in the interventricular foramina as well as the third ventricle, aqueduct of Sylvius, fourth ventricle, and foramen of Magendie (Fig. 3). Ventriculomegaly was felt to be secondary to cerebral atrophy and not to obstruction.

One patient had a large thalamic glioma displacing the posterior recesses and body of the third ventricle anteriorly (Fig. 4). The third ventricle was shifted to the right, and the posterior portion was markedly compressed. The tumor invaginated the third ventricle, almost covering the region of the iter. Moderate hydrocephalus was present without interstitial edema. Despite the effects of the mass, the CFVS was present in the aqueduct of Sylvius, indicating that it was not

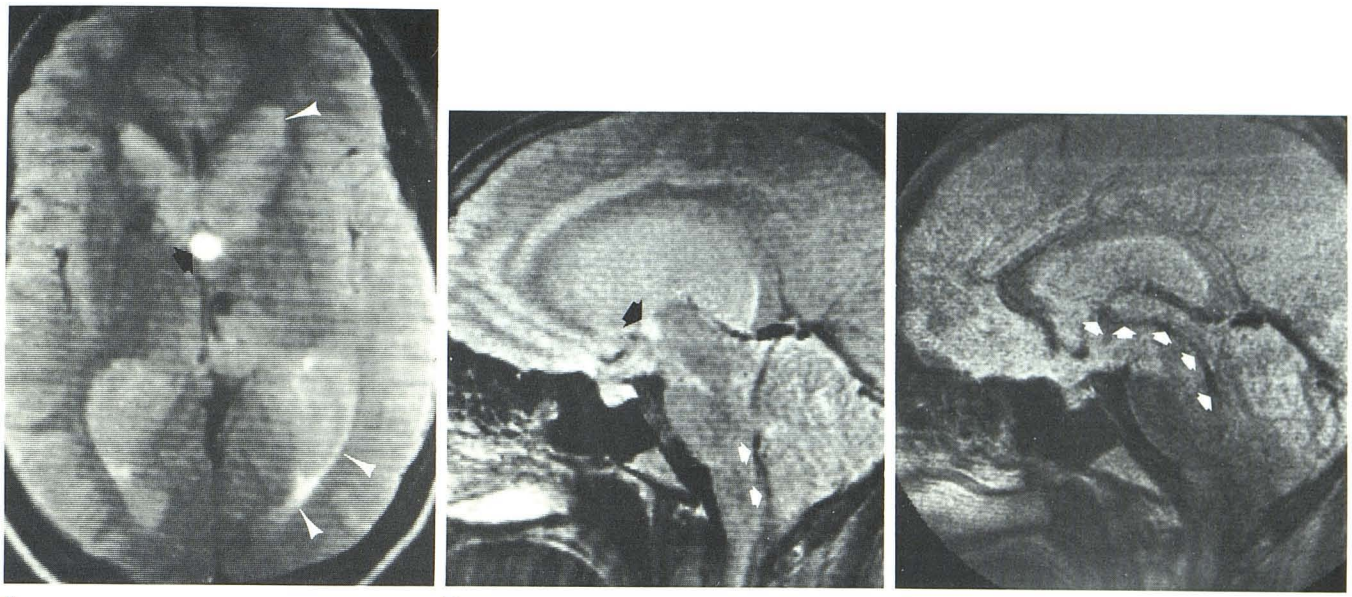

Fig. 1.—Colloid cyst obstructing interventricular foramina. **A**, SE 2500/80 transaxial image. Colloid cyst (*arrow*) is located slightly to right. CSF in ventricles is bright. Mild interstitial edema is present (*arrowheads*). (Round black focus to left of internal cerebral vein is an artifact.) **B**, SE 2400/80 sagittal image through level of aqueduct of Sylvius. 5-mm section thickness. CFVS is not seen in aqueduct on this image or on contiguous images. Colloid cyst is evident (*black arrow*). CFVS is present in caudal fourth ventricle and foramen of Magendie (*white arrows*). **C**, SE 2400/80 midline sagittal image obtained 2 months after removal of colloid cyst. Ventricular size has decreased. CFVS is now seen in interventricular foramina, third ventricle, and aqueduct of Sylvius (*arrows*). Contiguous image showed CFVS in foramen of Magendie.

Fig. 2.—Hypothalamic glioma obstructing anterior third ventricle and interventricular foramina. Midline sagittal images. **A**, SE 500/40. Mass is evident (*arrows*). **B**, SE 2400/80. CSF in aqueduct of Sylvius is bright (*arrows*). Absence of aqueductal CFVS is probably due to obstruction at more rostral level, but aqueductal obstruction cannot be excluded.

obstructed. The CFVS was also present in the interventricular foramina, the fourth ventricle, and foramen of Magendie.

Group 2. 14 Patients with Lesions Affecting the Aqueduct of Sylvius

None of the patients in this group had the CFVS in the aqueduct of Sylvius or third ventricle, although it was present in the caudal fourth ventricle in five patients. One patient with aqueductal stenosis had evidence of the CFVS in the interventricular foramina. Interstitial edema was only present in the patient with an obstructing sarcoid granuloma and resolved following placement of a shunt.

The four patients who had been shunted in childhood had only mild hydrocephalus. One of these patients, a 25-year-old woman, had dilatation of the fourth ventricle but without visualization of the CFVS in the foramen of Magendie (Fig. 5). The fourth ventricle was enlarged but was normally shaped. The CFVS was present in the left foramen of Luschka. This patient had been shunted at age 10 years. At the time of MR, she had symptoms of headache and vertigo. The appearance of the fourth ventricle is compatible with secondary fourth ventricular dilatation due to partial outlet obstruction or a Dandy-Walker variant [6].

Of the two patients with aqueductal stenosis recognized in adulthood, one with severe hydrocephalus was shunted (Fig.

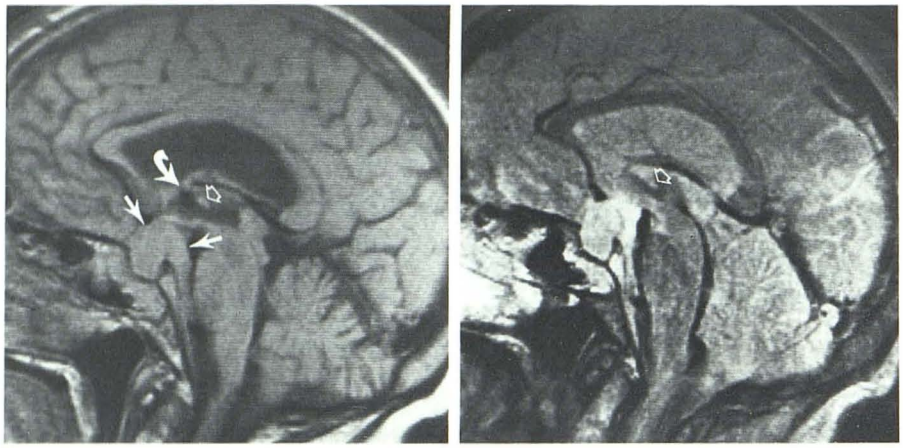

Fig. 3.—67-year-old woman with recurrent meningioma elevating anterior third ventricle. Sagittal images. **A**, SE 500/40. Mass is evident (*arrows*). CFVS is seen in interventricular foramina (*curved arrow*). **B**, SE 2400/80. CFVS extends through third ventricle, aqueduct of Sylvius, fourth ventricle, and foramen of Magendie. Interventricular foramina seen on contiguous image. Massa intermedia (*open arrow*) outlined by decreased intensity of the CFVS. Ventriculomegaly is due to atrophy.

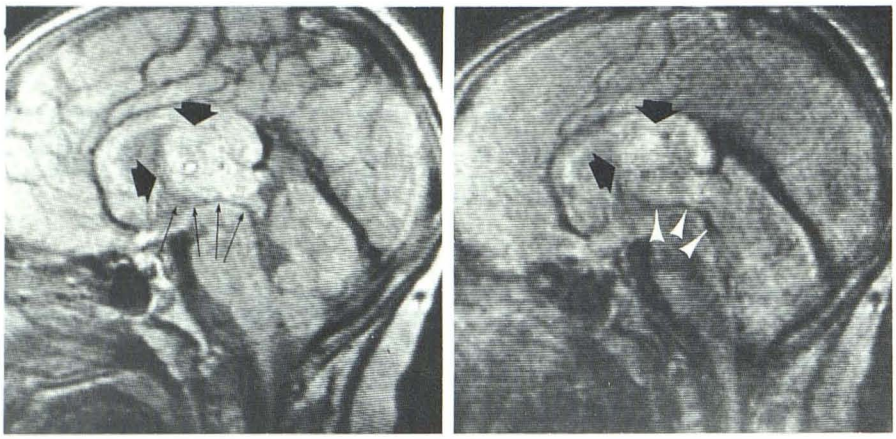

Fig. 4.—7-year-old boy with biopsy-proven thalamic glioma (*large arrows*) invaginating third ventricle and left lateral ventricle. Midline sagittal images. **A**, SE 1700/30. Note compressed posterior third ventricle and rostral aqueduct of Sylvius near iter (*small arrows*). **B**, SE 1600/100. Presence of CFVS (*arrowheads*) indicates that mass has not obstructed these areas.

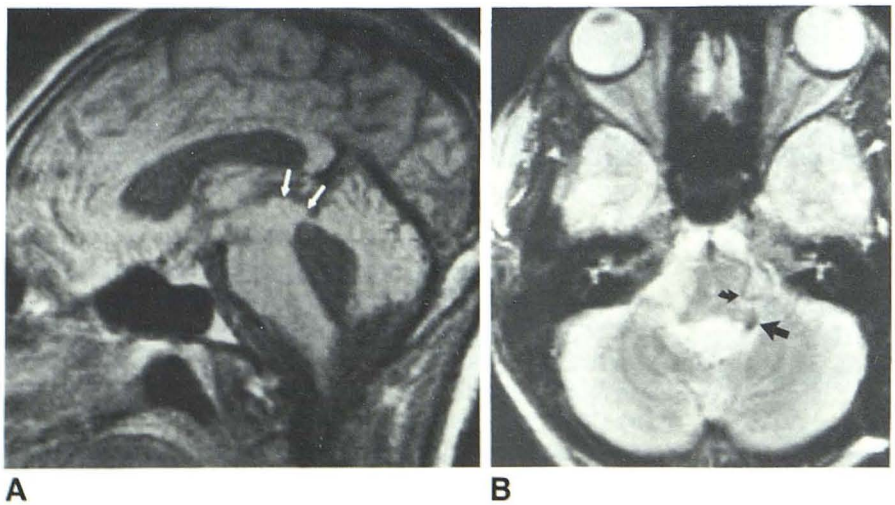

Fig. 5.—25-year-old woman. Aqueductal stenosis and possible "isolated" fourth ventricle. Treated since age 10 by ventriculoperitoneal shunting of lateral ventricles. **A**, SE 500/40. 10-mm-thick midline sagittal section. Aqueduct is not seen. Quadrigeminal plate is shown by *arrows*. Fourth ventricle is dilated. **B**, SE 2800/80. 10-mm-thick transaxial section. CFVS in left foramen of Luschka (*straight arrow*). Floccular loop of anterior inferior cerebellar artery is shown by *curved arrow*. Contiguous sections failed to demonstrate CFVS in foramen of Magendie.

6) and the other with moderate, compensated hydrocephalus was being followed closely but has refused the shunting procedure to date.

The three patients with probable tumors obstructing the aqueduct had moderate hydrocephalus. The tissue diagnosis is unknown in all three cases. In two of these patients the tectal plates appeared enlarged and brighter than the adjacent brain on SE 2500/80 sequences. The aqueduct in both pa-

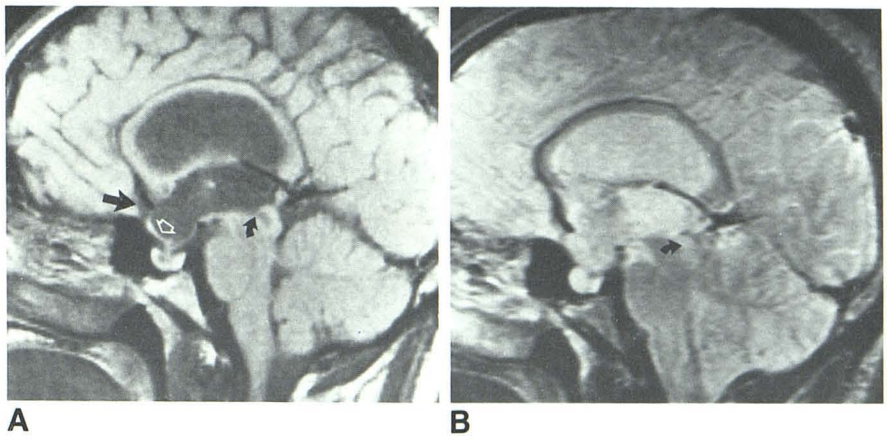

Fig. 6.—Aqueductal stenosis. 26-year-old man. Midline sagittal images. Section is 5 mm thick. Small fourth ventricle. Dilated lateral and third ventricles. **A**, SE 500/40. Rostral segment of aqueduct of Sylvius is dilated (*curved arrow*). Lamina terminalis is bowed anteriorly (*black arrow*). Optic chiasm is depressed (*open white arrow*). **B**, SE 1700/100. CSF in aqueduct of Sylvius is bright (*arrow*). CFVS is seen only in the caudal fourth ventricle and/or foramen of Magendie.

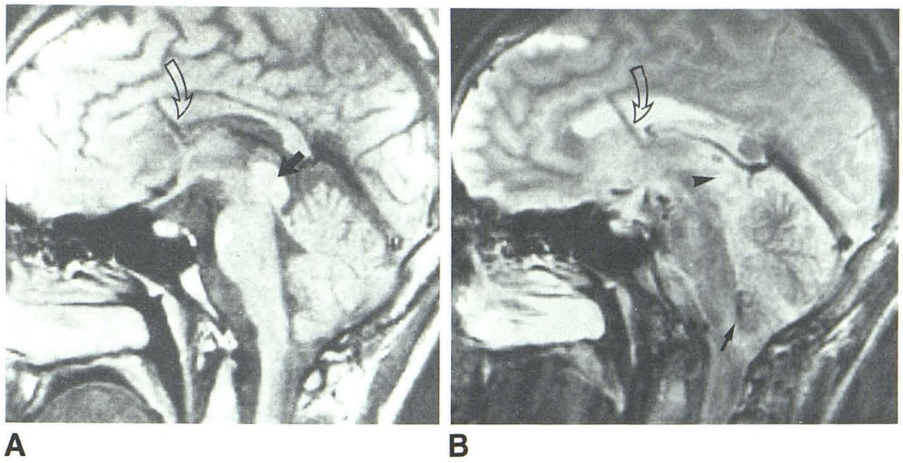

Fig. 7.—Probable tumor of mesencephalic tectum (not proven). Shunt tube indicated by *open arrow*. Midline sagittal images. Section is 5 mm thick. **A**, SE 500/40. Enlarged quadrigeminal plate (*black arrow*) compressing aqueduct of Sylvius. **B**, SE 2600/80. Note bright area in superior colliculus (*arrowhead*). Decreased intensity near foramen of Magendie probably represents CFVS and posterior inferior cerebellar artery (*small arrow*).

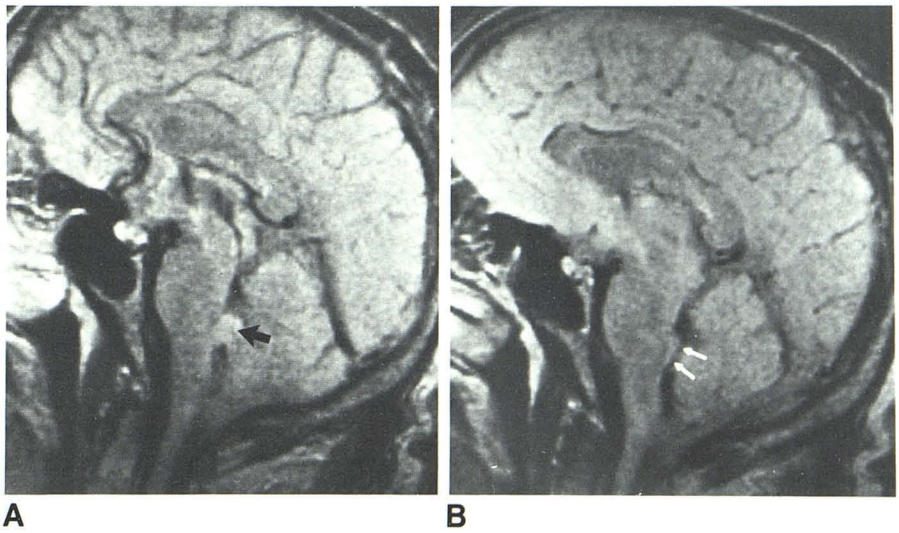

Fig. 8.—Choroid plexus papilloma of fourth ventricle. No hydrocephalus. SE 2200/60. 5-mm-thick contiguous sagittal images. **A**, Papilloma (*arrow*). CFVS is seen in interventricular foramina, third ventricle, aqueduct of Sylvius, fourth ventricle, and foramen of Magendie. **B**, Note CFVS coursing around the papilloma (*small white arrows*). No obstruction of CSF flow is present.

tients appeared circumferentially constricted on the SE 500/40 sequences. One of these patients has been shunted and has been followed by CT for 5 years without an observable change in the tectum (Fig. 7), while the other has been followed by CT for 3 years without change. The third patient has a presumed tumor of the tegmentum compressing the aqueduct. This 15-year-old patient with neurofibromatosis has had very minor symptoms for over 5 years and the parents

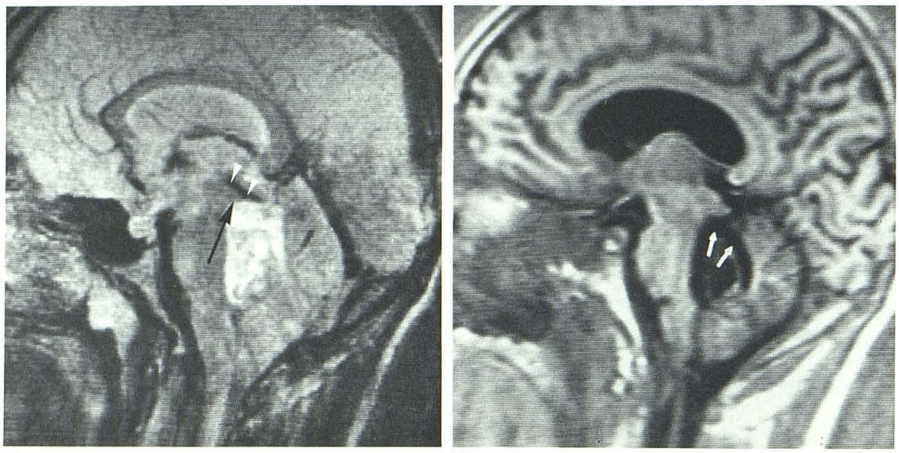

Fig. 9.—Astrocytoma of superior vermis and fourth ventricle. **A**, SE 2500/80. Midline sagittal image. Tumor is difficult to separate from surrounding CSF. Quadrigeminal plate is elevated (*black arrow*) but aqueductal CFVS is present (*white arrowheads*) indicating lack of obstruction and free communication with CSF in fourth ventricle. CFVS is present in interventricular foramina and possibly in foramen of Magendie. **B**, IR 2500/500. 6–7-mm lateral to midline. CSF can be seen around the tumor (*arrows*).

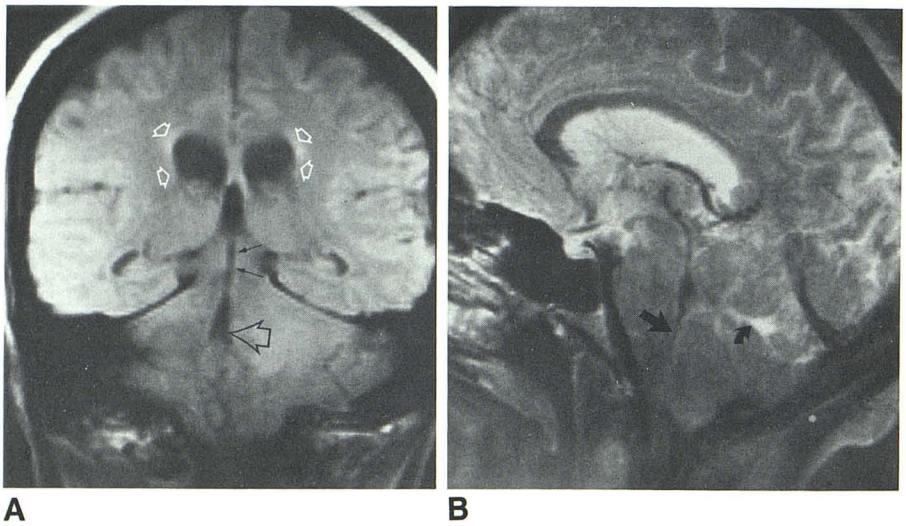

Fig. 10.—Metastasis to cerebellum from lung carcinoma. **A**, SE 1500/30. Coronal image. Fourth ventricle (*open black arrow*) is compressed and deviated to the right by tumor in left cerebellar hemisphere. Aqueduct is indicated by *small arrows*. Interstitial edema around lateral ventricles (*open white arrows*). **B**, SE 2500/80. Midline sagittal image. CFVS is present in posterior third ventricle, aqueduct of Sylvius, and body of fourth ventricle. Vasogenic edema in cerebellum (*curved arrow*). Caudal fourth ventricle is compressed (*straight arrow*). CFVS is not present in foramen of Magendie.

have refused surgical intervention or radiation therapy. The absence of the aqueductal CFVS on T2-weighted scans, and the failure to visualize the aqueduct of Sylvius on T1-weighted scans, indicates that there is complete or nearly complete aqueductal obstruction. The lack of interstitial edema [7] and presence of moderate hydrocephalus supports the clinical diagnosis of a long-standing lesion with compensated hydrocephalus.

Group 3. Seven Patients with Lesions Affecting the Fourth Ventricle

Two of these seven patients had mild hydrocephalus and intraventricular tumors that distorted the CFVS but did not obliterate it. In the patient with a small choroid plexus papilloma (Fig. 8), the CFVS was present in the fourth ventricle, coursing laterally around the mass, and was also seen in the interventricular foramina, the aqueduct, and the third ventricle. In the second patient with an intraventricular tumor, the aqueduct was elevated by an astrocytoma of the fourth ventricle and vermis, but the CFVS was still present in the aqueduct of Sylvius and in the caudal fourth ventricle and/or foramen of Magendie (Fig. 9). A prominent CFVS was present in the foramen of Magendie. The tumor could be more easily distinguished from the CSF with an inversion recovery sequence. The surgeon confirmed the patency of the aqueduct and reported that CSF flowed freely around the tumor, which was adherent only in the area of the roof of the fourth ventricle.

One patient had a large acoustic neuroma that obliterated the CFVS in the fourth ventricle although it was present in the aqueduct. Moderate hydrocephalus was present. After partial surgical resection of the neuroma, the CFVS was seen in the fourth ventricle as well as the aqueduct. Hydrocephalus decreased postoperatively, corroborating the reestablishment of CSF pathways.

One patient had a large hemangioblastoma that compressed the fourth ventricle and distal aqueduct, causing moderate hydrocephalus with interstitial edema. There was no evidence of the CFVS in this patient.

TABLE 2: **The CFVS Occurrence According to Ventricular Size**

Location of CFVS	Degree of Ventriculomegaly			
	None (n = 46)	Mild (n = 16)	Moderate (n = 15)	Severe (n = 9)
F. Monro		4 (24%)	5 (27%)	5 (56%)
Third ventricle	2 (4%)	10 (63%)	11 (75%)	7 (78%)
Aqueduct	31 (67%)	16 (100%)	15 (100%)	9 (100%)
Fourth ventricle	15 (32%)	15 (94%)	14 (93%)	9 (100%)
F. Magendie	18 (39%)	8 (50%)	11 (73%)	7 (78%)

Note.—Compilation of data [1, 22] on the visualization of the CSF flow-void sign on T2-weighted spin-echo pulse sequences (TR = 1500–4000 msec, TE = 60–100 msec). Categorization of ventricular size was made using the ventricular size index (see Table 1). Note the increasing likelihood of observing the CFVS as ventricular size increases.

One patient had a well-demarcated tumor of the brainstem with calcification but without surrounding edema. The tumor caused displacement of the aqueductal CFVS but did not obliterate the sign. The CFVS was also present in the caudal fourth ventricle. Only mild hydrocephalus was present. This patient is being followed, but the tissue diagnosis is unknown.

A patient with the Chiari II malformation had compression of the fourth ventricle and probably of the distal aqueduct. There was no evidence of the CFVS in any part of the CSF space. Moderate hydrocephalus was present but without interstitial edema. The patient is being followed for future consideration of intraventricular shunting.

Two patients with a lung metastasis to the cerebellum had edema and mass effect that obstructed the fourth ventricular outflow foramina, causing moderate dilatation of the entire ventricular system. Interstitial edema was present. In one case the CFVS was visible in the aqueduct of Sylvius on 10-mm axial scans, but it was not seen on 10-mm sagittal scans, possibly because of a positioning error. It was not seen elsewhere in the ventricular system. In the other patient, the CFVS was present in the third ventricle, aqueduct of Sylvius, and fourth ventricle. The caudal aqueduct of Sylvius and fourth ventricle were deviated slightly by edema from the cerebellar hemispheric lesion (Fig. 10).

Discussion

CSF is formed at the rate of 0.4 ml/min and moves from sites of formation to sites of absorption [8]. The rate of bulk flow is too slow to be a factor in the MR appearance of CSF. However, vigorous CSF pulsations are produced in the ventricular system, driven primarily by the systolic expansion of the cerebral vasculature [9–11]. These pulsatile movements produce turbulence and rapid flow of CSF through the narrower areas of the ventricular system, resulting in the loss of signal known as the CFVS [1]. Flow-dependent effects in the presence of magnetic field gradients have been described [12–16]. Flow-dependent MR effects have been shown in both conventional [17] and specialized pulse sequences [18]. On current MR imagers these effects can be manifested as time-of-flight effects, spin-phase shift effects, or as a combination of both, as is the case in conventional 2D FT SE sequences [16, 17]. The signal loss represented by the CFVS is probably caused by a combination of phase shift and time-of-flight effects. Spin-phase effects are valid for motion of spins in the imaging plane or through the imaging plane and are thus equally well seen in transverse, coronal, and sagittal images. Turbulence, whether due to high velocity or intrinsic physiological movements, results in large spatial variations of the spins within the imaging plane, causing spin-phase changes. The phase-encoding gradient is much weaker than the section-selection or read-out gradients, and thus the orientation of the phase-encoding gradient has little effect on the appearance of the CFVS. The technical explanations of time-of-flight and spin-phase effects have been more thoroughly analyzed by others [16, 19–21].

Recognition of the CFVS is useful because it confirms the patency of the area in which it is present. This is an important observation in patients with masses affecting CSF pathways, and provides a sensitive sign for comparison in follow-up examinations. In our patient with a thalamic tumor, the presence of the CFVS in the posterior third ventricle and aqueduct of Sylvius clearly indicated patency of these areas despite the distortion caused by the tumor (Fig. 4). It was also helpful in the patient with a recurrent meningioma bulging into the anterior third ventricle, in which a prominent CFVS was present in the interventricular foramina (Fig. 3). This patient will be followed with MR, and the loss of the CFVS in the interventricular foramina will be considered an early sign of obstruction at that level.

The significance of the absence of the CFVS is variously interpreted, depending on the location in the ventricular system and the degree of hydrocephalus that is present. The degree of hydrocephalus has a significant effect on the visualization of the CFVS, and an important distinction must be made between patients without hydrocephalus or with mild hydrocephalus and patients with moderate or severe hydrocephalus. Previously reported data on the visualization of the CFVS in patients with normal and enlarged ventricles are summarized in Table 2 [1, 22]. The CFVS is most consistently seen in the aqueduct of Sylvius. In patients with ventriculomegaly (graded according to the ventricular size index in Table 1) due to atrophy and/or extraventricular obstructive hydrocephalus, the CFVS was present in the aqueduct of Sylvius in all 40 patients in the study [22], while it was present in the aqueduct in only 67% (31/46) of patients with normal MR examinations [1]. By contrast, the CFVS was present in the third ventricle in only 4% of normal patients (2/46) but was present in 78% (7/9) of patients with severe ventriculomegaly. The CFVS was seen in the foramina of Monro in 25% (4/16) of patients with mild ventriculomegaly but was present in 56%

(5/9) of patients with severe ventriculomegaly. The CFVS was visualized with certainty in the foramen of Magendie in 50% of patients with hydrocephalus and was probably present in many more patients but could have been confused with the posterior inferior cerebellar arteries [1, 22].

We found that the absence of the aqueductal CFVS correlated well with the presence of an obstruction (Figs. 5 and 6) but did not always specifically localize the obstruction (Figs. 1 and 2). In one patient with a colloid cyst obstructing the interventricular foramina, the CFVS was seen only in the caudal fourth ventricle and foramen of Magendie (Fig. 1). After surgical removal of the colloid cyst the patient was restudied using identical pulse sequences. The CFVS was then seen coursing from the level of the interventricular foramina to the foramen of Magendie in an unbroken continuous stream.

In one patient who was shunted at age 10 for aqueductal stenosis, we observed cystic dilatation of the fourth ventricle. Blockages of the foramina of Luschka and Magendie and of the aqueduct of Sylvius have been described as the causative factors in cystic dilatation of the fourth ventricle, termed a "trapped" or "isolated" fourth ventricle [23, 24]. In the Dandy-Walker malformation, the foramina of Magendie and Luschka are atretic, while in the Dandy-Walker variant the vallecula is wide and hydrocephalus may not be present [6]. We observed an unusually prominent CFVS in the left foramen of Luschka but could not identify any decreased signal in the foramen of Magendie. The vallecula was small. Since the CFVS is more likely to be seen in patients with large CSF spaces (Table 2) [22], the absence of the foramen of Magendie CFVS in a patient with a dilated fourth ventricle is a more significant finding. We interpret these findings as representing probable partial fourth ventricular outlet obstruction with increased flow directed through one outlet foramen. The appearance is compatible with an "isolated" fourth ventricle, although it is difficult to exclude a Dandy-Walker variant. While most patients with an "isolated" fourth ventricle have posterior fossa signs clinically, Scotti et al. reported that it can also be seen in asymptomatic patients [24]. Our patient had only mild symptoms. It may be that the asymptomatic patients have only partial outlet obstruction.

Observing whether the CFVS is present or absent is especially useful for patients in whom aqueductal obstruction is suspected. Previous reports of the MR appearance of aqueductal stenosis have emphasized the disparity in the sizes of the dilated lateral and third ventricles as compared with a normal or small fourth ventricle and the absence of obstructing tumors [25–27]. The apparent patency of the aqueduct in the presence of lateral and third ventricular enlargement with a normal fourth ventricle has been interpreted as a sign of a membranous, rather than long-segment, stenosis of the aqueduct [25]. This can be misleading since 25–35% of patients with extraventricular obstructive hydrocephalus (formerly called communicating hydrocephalus) will show little or no dilatation of the fourth ventricle [28]. Some patients with this ventricular pattern do not have extraventricular obstructive hydrocephalus or aqueductal stenosis. The correct diagnosis can be made in these patients by observing the CFVS in the aqueduct or by a limited pneumoencephalogram showing free passage of air into the third ventricle. We previously reported one such patient [22] in whom we were able to confirm the pneumoencephalographic findings of aqueductal patency by using 5-mm T2-weighted sagittal and axial images (SE 2300/80). An initial study with 10-mm thick sections failed to demonstrate the aqueductal CFVS. Five-mm scans provide clearer depiction of the aqueduct on the T1-weighted images and may occasionally be necessary for identifying the aqueductal CFVS on the T2-weighted images. Observation of the CFVS overcomes the problem of volume-averaging of the aqueduct, which may cause an artifactually narrowed appearance, even on 5-mm thick sections.

The mere presence of a mass arising in or protruding into the ventricle does not eliminate the CFVS in all cases. We noted a "streaming" effect of CSF around a choroid plexus papilloma of the fourth ventricle (Fig. 8) and around a partially resected acoustic neuroma protruding into the fourth ventricle. In the latter patient, the CFVS was not seen on the preoperative MR, and obstructive hydrocephalus with interstitial edema was present. Following partial resection of the tumor the CFVS was seen in the posterior third ventricle, the aqueduct of Sylvius and through the entire fourth ventricle. The degree of hydrocephalus was decreased and the interstitial edema had resolved.

In a patient with an astrocytoma filling the fourth ventricle and extending into the superior vermis, the tectal plate was elevated but a prominent CFVS was present in the aqueduct. Inversion recovery images demonstrated CSF around the tumor. We felt that these findings indicated a lack of impedance to the flow of CSF around the tumor, thus pulsatile CSF movement through the aqueduct could be maintained. The surgeon found a smooth, glistening tumor filling the fourth ventricle and extending through the roof into the vermis. He confirmed the patency of the aqueduct and observed CSF flowing around the tumor, which was not adherent to the floor of the fourth ventricle.

In summary, the MR depiction of flow-related phenomena in the ventricular system provides dynamic information about the movement of CSF that has previously been obtainable only by ventriculography or pneumoencephalography. Unlike ventriculography and pneumoencephalography, the CFVS is a representation of true physiology, undisturbed by the changes in pressure that occur when the subarachnoid space is entered. The significance of the absence of the CFVS must be considered in relation to the size of the ventricles and with the knowledge that many normal patients do not exhibit the sign. However, we believe that the CFVS is an important diagnostic observation. The use of the CFVS in conjunction with the anatomic and tissue characterization information increases our understanding of the effect of tumors and other disease processes on the brain and the ventricular pathways.

ACKNOWLEDGMENT

Our thanks to J.A.S., Mary Anne Thomas, and Arlene Kisliuk.

REFERENCES

1. Sherman JL, Citrin CM. Magnetic resonance demonstration of normal CSF flow. *AJNR* **1986**;7:3–6

2. DeLaPaz RL, Davis DO, Norman D, O'Donohue J, Enzman DR. Cerebrospinal fluid motion effects in cerebral MR imaging. Presented at the 71st annual meeting of the Radiological Society of North America, Chicago, November **1985**
3. Bradley WG, Kortman KE, Burgoyne B. The effect of pulsatile flow on CSF intensity in MR imaging of the brain. Presented at the 71st annual meeting of the Radiological Society of North America, Chicago, November **1985**
4. TerBrugge KG, Rao KC. Hydrocephalus and atrophy. In: Lee SH, Rao KC, eds. *Cranial computed tomography*. New York: McGraw-Hill, **1983**:171–200
5. Chui KM, Blakesley DM, Mohapatra SN. Test method for MR image slice profile. *J Comput Assist Tomogr* **1985**;9:1150–1152
6. Rao KC, Harwood-Nash DC. Craniocerebral anomalies. In: Lee SH, Rao KC, eds. *Cranial computed tomography*. New York: McGraw-Hill, **1983**:115–169
7. Drayer BP, Rosenbaum AR. Brain edema defined by cranial computed tomography. *J Comput Assist Tomogr* **1979**:317–323
8. Cutler RW, Page L, Galicich J, Watters GV. Formation and absorption of cerebrospinal fluid in man. *Brain* **1968**;91:707–719
9. Portnoy HD, Bhopp M, Branch C, Shannon MB. Cerebrospinal fluid pulse waveform as an indicator of cerebral autoregulation. *J Neurosurg* **1982**;56:666–678
10. Du Boulay GH. Pulsatile movements in the CSF pathways. *Br J Radiol* **1966**;39:255–262
11. Citrin CM, Sherman JL, Gangarosa RE, Scanlon D. CSF flow-void sign: physiology and etiology. Presented at the 24th annual meeting of the American Society of Neuroradiology, San Diego, January **1986**
12. Singer JR. Blood flow rates by nuclear magnetic resonance measurements. *Science* **1985**;130:1652–1653
13. Battocletti JH, Linehan JH, Larsen SJ, et al. Analysis of a nuclear magnetic resonance blood flow for pulsatile flow. *IEEE Trans Biomed Eng* **1972**;BME-19:403–407
14. Moran PR. A flow velocity zeugmatographic interlace for NMR imaging in humans. *Mag Reson Imaging* **1982**;1:197–203
15. Waluch V, Bradley WG. NMR even echo rephasing in slow laminar flow. *J Comput Assist Tomogr* **1984**;8:594–598
16. von Schulthess GK, Higgins CR. Blood flow imaging with MR: spin-phase phenomena. *Radiology* **1985**;157:687–695
17. Wedeen VJ, Meuli RA, Edelman RR, et al. Projective imaging of pulsatile flow with magnetic resonance. *Science* **1985**;230:946–948
18. Le Bihan D, Breton E, Lallemand D, Grenier P, Cabanis E. Diffusion MR imaging: neurological results. Presented at the 71st annual meeting of the Radiological Society of North America, Chicago, November **1985**
19. Bradley WG, Waluch V. Blood flow: magnetic resonance imaging. *Radiology* **1985**;154:443–450
20. Crooks LE, Mills CM, Davis PL, et al. Visualization of cerebral and vascular abnormalities by NMR imaging. The effects of imaging parameters on contrast. *Radiology* **1982**;144:843–854
21. von Schulthess GK, Fisher MR, Crooks LE, Higgins CB. Gated MR imaging of the heart: intracardiac signals in patients and healthy subjects. *Radiology* **1985**;156:125–132
22. Sherman JL, Citrin CM, Bowen BJ. MRI demonstration of CSF flow in ventriculomegaly. Presented at the 71st annual meeting of the Radiological Society of North America, Chicago, November **1985**
23. Zimmerman RA, Bilaniuk LT, Gallo E. Computed tomography of the trapped fourth ventricle. *AJR* **1978**;130:503–506
24. Scotti G, Muscrage MA, Fitz CR, Harwood-Nash DC. The isolated fourth ventricle in children: CT and clinical review of 16 cases. *AJR* **1980**;135:1233–1238
25. Hueftle MG, Han JS, Kaufman B, Benson JE. MRI of brainstem gliomas. *J Comput Assist Tomogr* **1985**:263–267
26. Lee BCP, Kneeland JB, Deck MDF, Cahill PT. Posterior fossa lesions: magnetic resonance imaging. *Radiology* **1984**;153:137–143
27. Han JS, Bonstell CT, Kaufman B, et al. Magnetic resonance imaging evaluation of the brainstem. *Radiology* **1984**;150:705–712
28. Naidich TP, Schott LH, Baron RL. Computed tomography in the evaluation of hydrocephalus. *Radiol Clin North Am* **1982**;20:143–167